Focal Mechanism Solutions of the 2008 Wenchuan earthquake sequence from P-wave polarities and SH/P amplitude ratios: new results and implications

Citation: Tian, Yuan, Jieyuan Ning, Chunquan Yu, Chen Cai, and Kai Tao. "Focal Mechanism Solutions of the 2008 Wenchuan Earthquake Sequence from P-Wave Polarities and SH/P Amplitude Ratios: New Results and Implications." Earthq Sci 26, no. 6 (December 2013): 357–372.

As Published: http://dx.doi.org/10.1007/s11589-014-0067-y

Publisher: Seismological Society of China

Persistent URL: http://hdl.handle.net/1721.1/104040

Version: Author's final manuscript: final author's manuscript post peer review, without publisher's formatting or copy editing

Earthq Sci (2013) 26(6):357–372
DOI 10.1007/s11589-014-0067-y

RESEARCH PAPER

Focal Mechanism Solutions of the 2008 Wenchuan earthquake sequence from P-wave polarities and SH/P amplitude ratios: new results and implications

Yuan Tian · Jieyuan Ning · Chunquan Yu · Chen Cai · Kai Tao

Received: 30 August 2013 / Accepted: 8 January 2014 / Published online: 31 January 2014

Abstract The 2008 Wenchuan earthquake, a major intraplate earthquake with M_w 7.9, occurred on the slowly deforming Longmenshan fault. To better understand the causes of this devastating earthquake, we need knowledge of the regional stress field and the underlying geodynamic processes. Here, we determine focal mechanism solutions (FMSs) of the 2008 Wenchuan earthquake sequence (WES) using both P-wave first-motion polarity data and SH/P amplitude ratio (AR) data. As P-wave polarities are more reliable information, they are given priority over SH/P AR, the latter of which are used only when the former has loose constraint on the FMSs. We collect data from three categories: (1) permanent stations deployed by the China Earthquake Administration (CEA); (2) the Western Sichuan Passive Seismic Array (WSPSA) deployed by Institute of Geology, CEA; (3) global stations from Incorporated Research Institutions for Seismology. Finally, 129 events with magnitude over M_s 4.0 in the 2008 WES are identified to have well-constrained FMSs. Among them, 83 are well constrained by P-wave polarities only as shown by Cai et al. (Earthq Sci 24(1):115–125, 2011), and the rest of which are newly constrained by incorporating SH/P AR. Based on the spatial distribution and FMSs of the WES, we draw following conclusions: (1) the principle compressional directions of most FMSs of the WES are subhorizontal, generally in agreement with the conclusion given by Cai et al. (2011) but with a few modifications that the compressional directions are WNW–ESE around Wenchuan and ENE–WSW around Qingchuan, respectively. The subhorizontal compressional direction along the Longmenshan fault from SW to NE seems to have a left-lateral rotation, which agrees well with regional stress field inverted by former researchers (e.g., Xu et al., Acta Seismol Sin 30(5), 1987; Acta Geophys Sin 32(6), 1989; Cui et al., Seismol Geol 27(2):234–242, 2005); (2) the FMSs of the events not only reflected the regional stress state of the Longmenshan region, but also were obviously controlled by the faults to some extent, which was pointed out by Cai et al. (2011) and Yi et al. (Chin J Geophys 55(4):1213–1227, 2012); (3) while the 2008 Wenchuan earthquake and some of its strong aftershocks released most of the elastic energy accumulated on the Longmenshan fault, some other aftershocks seem to occur just for releasing the elastic energy promptly created by the 2008 Wenchuan earthquake and some of its strong aftershocks. (4) Our results further suggest that the Longmenshan fault from Wenchuan to Beichuan was nearly fully destroyed by the 2008 Wenchuan earthquake and accordingly propose that there is less probability for great earthquakes in the middle part of the Longmenshan fault in the near future, although there might be a barrier to the southwest of Wenchuan and it is needed to pay some attention on it in the near future.

Keywords Longmenshan fault · Wenchuan earthquake sequence · Focal mechanism solutions · Stress

Y. Tian · J. Ning (✉) · K. Tao
Institute of Theoretical and Applied Geophysics, School of Earth and Space Sciences, Peking University, Beijing 10086, China
e-mail: njy@pku.edu.cn

C. Yu
Department of Earth, Atmospheric and Planetary Sciences, MIT, Cambridge, MA 01239, USA

C. Cai
Department of Earth & Planetary Sciences, Washington University, Saint Louis, MO 63130-4899, USA

1 Introduction

On 12 May 2008, a great earthquake with magnitude M_w 7.9 occurred in Longmenshan fault belt, Sichuan province. This great event and its strong aftershocks caused enormous loss of life and catastrophic damage of infrastructure (Zhang et al. 2008; Burchfiel et al. 2008). To mitigate disasters caused by great earthquakes in this region in the near future and reveal the geodynamic feature of the Longmenshan area, it is necessary to fully understand the source properties and triggering mechanisms of the 2008 Wenchuan earthquake sequence (WES), as well as the stress field in the Longmenshan area.

The 2008 Wenchuan earthquake (the mainshock of the 2008 WES) is considered to be initiated on Yingxiu-Beichuan fault and then propagated northeastward on a surface rupture zone of about 220 km long on the Yingxiu-Beichuan-Qingchuan fault and 70 km long on the Anxian-Guanxian-Jiangyou fault (Lin et al. 2009; Liu-Zeng et al. 2009, 2010; Xu et al. 2009). These faults were relatively quiescent in seismicity (Loveless and Meade 2011; Meade 2007). Source inversions based on teleseismic data showed a pattern of double-peak energy release during rupture (e.g., Ji and Hayes 2008; Nakamura et al. 2010; Zhang and Ge 2010; Zhang et al. 2009). The first peak was near Yingxiu-Hongkou, Wenchuan about 10–20 s after the initial burst, and the second energy peak came 50 s later near Beichuan. The largest thrust slip is found on the moderately dipping thrust fault near Yingxiu-Hongkou and the largest strike slip is located near Beichuan (e.g., Shen et al. 2009; Wang et al. 2011).

Hu et al. (2008) preliminarily determined 44 FMSs of strong aftershocks using P-wave first-motion polarities (PWFMP) and a revised Grid Search Method named CHNYTX (Yu et al. 2009). Soon later, Wang et al. (2009) obtained 88 moment tensor solutions. Zheng et al. (2009) also determined the FMSs of 10 biggest aftershocks with magnitude $M_s \geq 5.6$ employing the Cut-And-Paste (CAP) method. Later on, they further showed FMSs of 18 aftershocks with magnitude $M_s \geq 5.0$ employing the same technique (Zheng et al. 2010). Cai et al. (2011) provided 83 well-determined FMSs. Above results showed that most of the strong aftershocks were thrust events, of which some were similar to the main shock, while others were not. They also claimed that there were many strike-slip events. When their results provided a preliminary sight of the aftershock pattern of the 2008 WES, limited number of FMSs prevented them from showing comprehensive expression of the regional stress state. For further validating these results and fully understanding their geodynamic implications, it is necessary to give more well-determined FMSs.

Recently, Yi et al. (2012) determined 312 FMSs employing the CAP method. Instead of analyzing those FMSs one by one, they statistically analyzed then and got some statistical conclusions. Although statistical analyses have advantage on showing objective conclusions, one by one analyses are still needed because they might show detailed information and help us to fully understand the results and implications. Furthermore, it is also necessary to take those poorly constrained ones in analyses, because the poorly constrained events might contain special information on fault activity.

In this paper, we will first use P-wave first-motion polarities to determine P-wave FMSs. Then, we will include the amplitude ratios (AR) of SH-wave to P-wave at local stations to help us further constrain those solutions. Accordingly, we will give a detailed discussion on the obtained results. At last, we will discuss triggering mechanisms of various types of FMSs as well as their implications for the regional stress field in the Longmenshan area.

2 Data and methods

P-wave first-motion polarity (PWFMP) is well-defined signal that suffers little influence from mechanical properties of the media. With enough high quality polarity data, one may obtain the FMSs with enough confidence. Various methods have been developed to determine the P-wave first-motion FMSs (Kasahara 1963; Brillinger et al. 1980; Xu et al. 1983; Reasenberg and Oppenheimer 1985; Hardebeck and Shearer 2002). Yu et al. (2009) refined the method and showed a new grid search program of calculating P-wave first-motion FMSs (CHNYTX), which was published on http://geophy.pku.edu.cn/itag/node/application.php. Compared with some other grid search programs such as HASH (Hardebeck and Shearer 2002) and the grid search method (Xu et al. 1983), this program has many improvements. First, it determines the weight of P-wave polarity observations not only based on their quality but also their distribution density on the focal sphere. Second, it employs jackknife technique to improve the inversion quality, which may reduce the possibility that the solution is biased by a wrong polarity. Third, it has employed new principles of clustering the possible solutions so that it could give at most three possible cluster centers. Finally, it provides a more reasonable scheme for evaluating the quality of FMSs.

Compared to former grid search programs, CHNTYX has better performance on those events with sparse or unevenly distributed P-wave first-motion observations. However, while Yu et al. (2009) showed that at least one cluster of possible solutions of an event should be very close to the true solution, the new program still needs more knowledge to determine which one is right when there are more choices. Here, we try to employ AR of SH-wave to

P-wave to help us evaluate which cluster of those choices for an event is closest to its true FMS.

Theoretically, it only needs 5–6 high quality AR observations to obtain a FMS when using AR method individually (Kisslinger 1980; Kisslinger et al. 1981). Compared with using P- or S-wave amplitude alone, the AR method is more superior as it may reduce the influence of source time function and ray path. But, AR method has its own drawbacks. Noise in waveforms can lead to scatter in the S/P ratios of a factor of 2, sometimes up to a factor of 5 (Rau et al. 1996; Nakamura et al. 1999; Hardebeck and Shearer 2003). Conventionally, an observation would be deleted if the difference between the theoretical and observed S/P ratios is large (Kisslinger et al. 1981; Hardebeck and Shearer 2003).

Significant large scatter in SH/P ratio mostly happens around the nodal planes as a result of near-zero P-phase amplitude and in fact offers a good constraint for the true FMS. Accordingly, instead of taking AR observations into inversion, we plot SH/P ratio observations of an event on a colored beach ball with their colors representing theoretical ratios, and then pick out the correct cluster manually from those possible solutions given by CHNTYX. In this way, AR ratio data perfectly serve as complement to the PWFMP data, resulting in both high quality and more FMSs. We should mention that SV to P AR is not applied in our study because the amplitude of SV wave is more difficult to measure as it might be contaminated by the P-coda wave (Kisslinger et al. 1981).

Figure 1 shows an example that tells how we use AR to select the preferred FMS from a group of possible solutions given by CHNTYX. In this example, the P polarity observations are not well distributed so that the CHNYTX gives three cluster centers of possible solutions as were shown in Fig. 1a1. The SH/P ratio distributions for different possible solutions are shown in Fig. 1a2–a4. Colors of the beach ball express the theoretical logarithm of SH/P ratio with red color showing large ratios and blue color showing small. Black circles are the observed AR. We could see that both stations L0203 (Fig. 1b4) and KMY03 (Fig. 1b1) have very small Pg and relatively large SH, which indicate that they should be located near the nodal planes. Contrarily, stations L0207 (Fig. 1b2) and L0204 (Fig. 1b3) have very sharp Pg and relatively small SH, indicating that they should be in the blue areas far from the nodal planes. Figure 1a3, a4 clearly shows that the two solutions shown in a1 by black and green lines are unconvincing, while the solution given in Fig. 1a2 fits the SH/P values best and will be our final solution.

We collect P-wave polarities and SH/P AR from three categories. The first part of data comes from the Chinese Earthquake Administration (CEA). Most of CEA stations are regional permanent stations, and others are the temporary stations installed along the Longmenshan fault a few days after the main shock of WES (Zheng et al. 2010). The second part comes from the Western Sichuan Passive Seismic Array (WSPSA) deployed by Institute of Geology, CEA (Liu et al. 2008). As some of WSPSA stations were very close to the Longmenshan fault, they offered plenty of AR data as well as a good complement to the Pg observations used in CHNYTX.

The third part of observations comes from remote stations and is downloaded from the website of Incorporated Research Institutions of Seismology (IRIS, http://www.iris.edu/gmap). The distribution of CEA and WSPSA stations as well as some IRIS stations located in the span area of CEA stations are all shown in Fig. 2. Generally speaking, three group of observation stations are fairly distributed and form good constraints on FMSs.

Totally, 129 events with magnitude over M_s 4.0 in WES are identified to have unique FMSs. All of them are shown in Fig. 3. Their characteristics and implications will be discussed in the following parts of this paper. However, there are still many events not well constrained. For comprehensively understanding the stress field in this region, we include poorly constrained events with magnitude over 5.0 in our discussion.

3 Results

3.1 FMSs of the events with $M_s > 5.0$

There are 65 events with magnitude over 5.0 in total. 14 of these events lack clear P polarity observations or have poor signal-to-noise ratio (SNR) roughly due to contamination from previous event's code wave. For instance, 11 events happened in the first 3 h after the main shock, while other three events are affected by some events that occurred right before them [e.g., event 133150542 (31.22°N, 103.47°E, M_s 5.2) happened only 13 s after a large nearby event 133150529 (31.25°N, 103.57°E, M_s 5.1) with similar location and magnitude]. The other 51 events have more than 10 clear P polarity observations that allow us to calculate their FMSs. After applying AR data, 42 of them have well-determined FMSs.

We have carefully checked the waveforms of the other nine events with poorly constrained solutions, trying to find out what are the possible causes of low quality. There are two events (137161442, No. 207 in Fig. 4; 206070928, No. 208 in Fig. 4) with two cluster centers which are similar to each other. In this case, either of the two centers or their average could be regarded as the real FMS. For each of the other seven events, their cluster centers are separated. Among them, five events have unevenly distributed polarity observations, leaving large gap on the focal

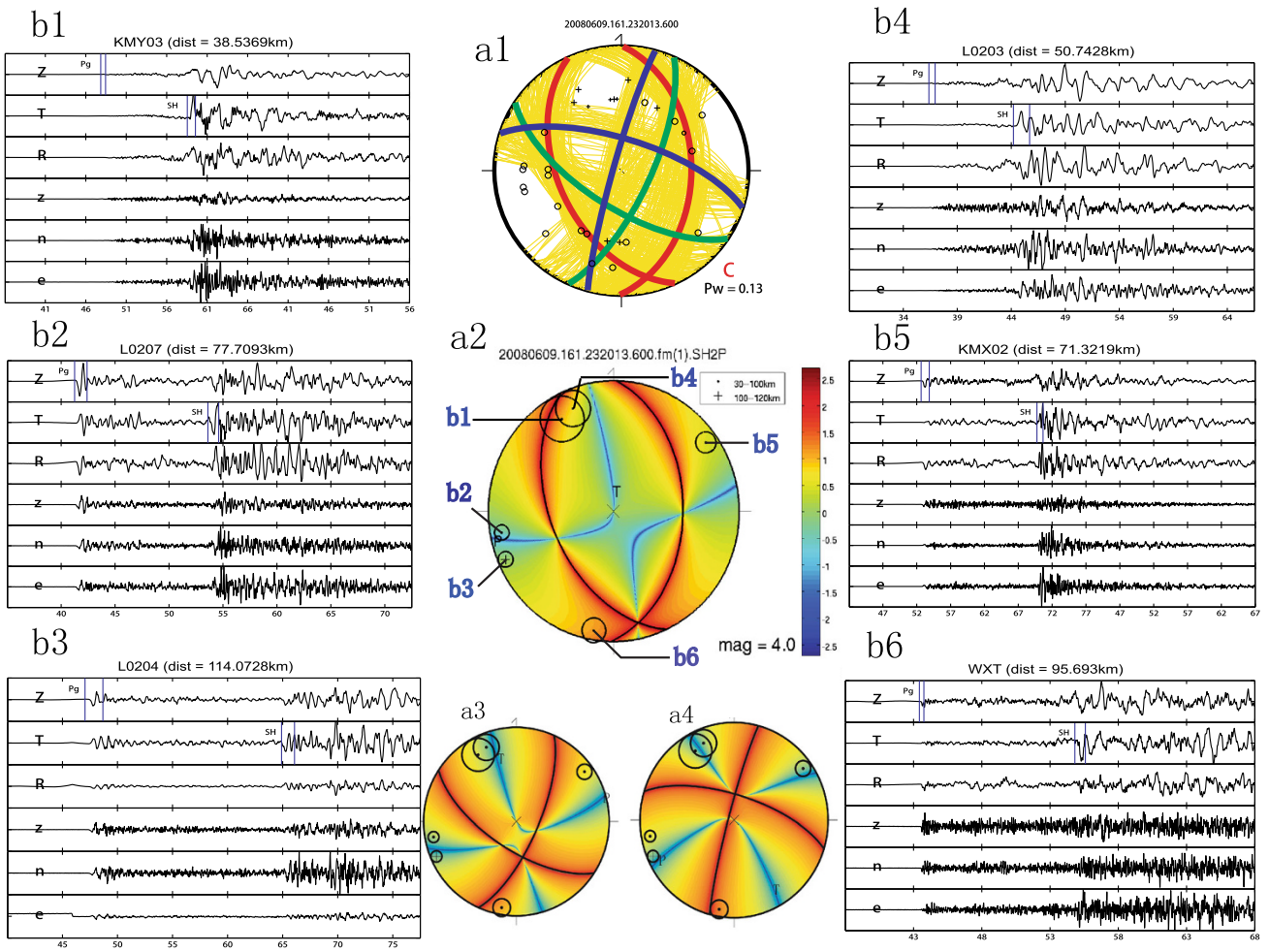

Fig. 1 An example shows how to use AR to select the right FMS from possible solutions given by CHNTYX. **a1** Solutions obtained by the P-wave first-motion polarities. **b1–b6** are the records we use. All station records satisfy: (1) have the epi-distance less than 120 km (mostly less than 100 km); (2) have clear Pg wave and (SH)g wave. The three-component seismograms (the lower three trances in **b1–b6**) are filtered with a 0.2–15 Hz window and then rotated to vertical (*Z*), radial (*R*), and tangential (*T*) components (upper three traces in **b1–b6**). Note that all three components shown in Fig. 1 have been normalized. Free surface correction has also been applied to the measured AR. The theoretical (SH/P) ratios are shown by the *color images* in the beach balls, and the observations are plotted as *circles* at the piercing points. **a2** is the solution which fits the (SH/P) ratio best. **a3** and **a4** are the other two solutions given by P polarity but poor

spheres. At the same time, there are not enough direct Pg wave polarities with large take-off angles, especially for the events occurred in the northern part of Longmenshan fault zone. We give our own preference for these five events under some principle. If SH/P AR are available, we will choose the solution that fits the AR better. If there are few AR observations, we will compare the waveforms of those events with nearby events which already have well-determined FMSs. If they share similar waveforms, we will choose the cluster centers close to the nearby events' FMSs for reference. The events belonging to this category are shown in Fig. 4 with Nos. 201, 202, 203, 204, and 206.

There are still 2 events remaining with very confusing distribution of P polarity observations (135055456, Nos. 205; 225210320, No. 209). The polarities of event No. 205 from stations in SW back azimuth seem not to be consistent with each other. It appears to have both up-going and down-going Pn polarities. If we separate those polarity observations by distance, we could see that polarities change regularly with distance. Concretely speaking, stations with epi-distance about 100–200 km show down-going Pn polarities while stations with epi-distance more than 230 km show up-going polarities. The FMS and seismograms of event No. 205 are shown in Fig. 5. We could see clearly that both the waveform and polarity of the first arrival signals from stations within 100–200 km epicentral distances are quite different from those of stations over 200 km away. This might imply that in the crust of the southern part of Longmenshan belt there might be a relatively sharp velocity interface (the Conrad discontinuity for instance), where some new phases

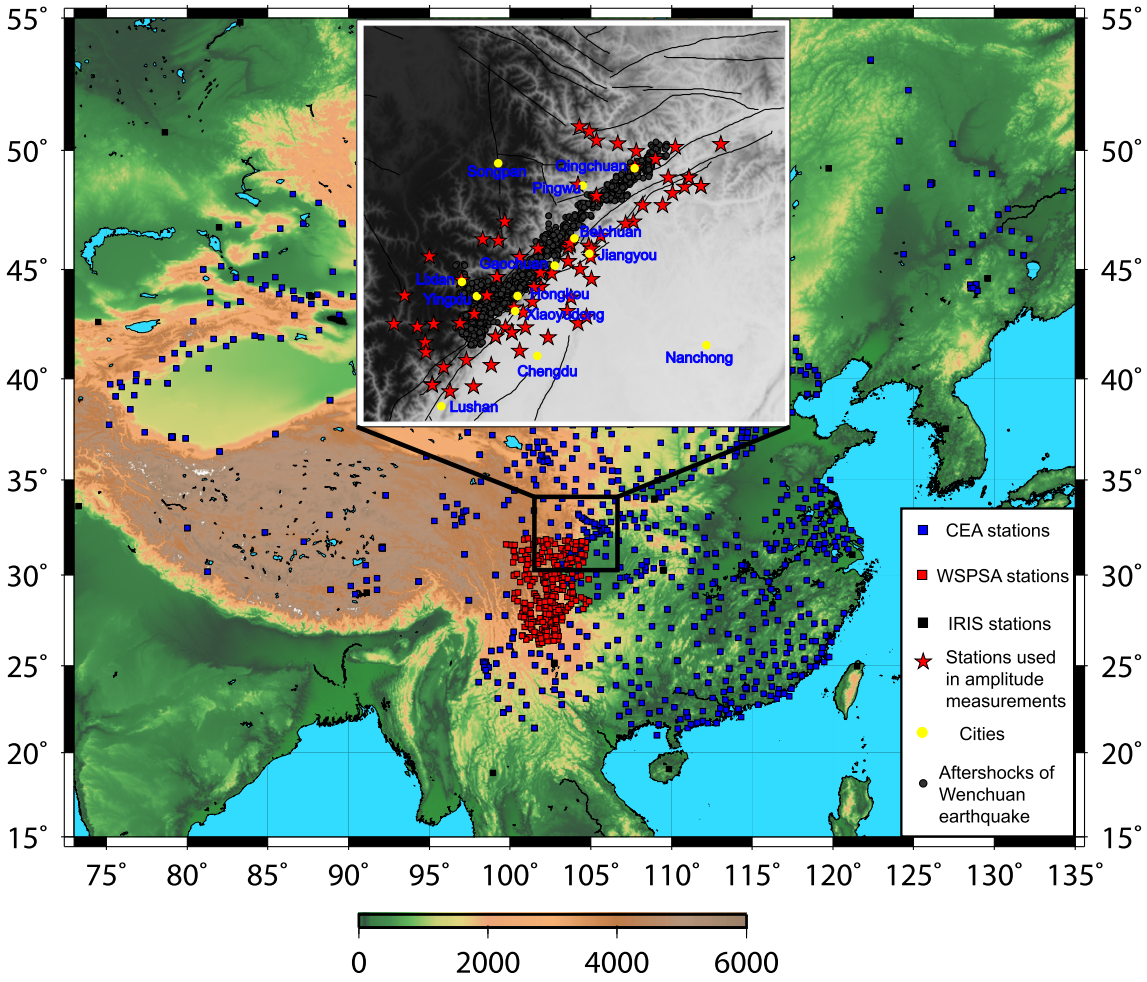

Fig. 2 Spatial distribution of the aftershocks of the 2008 Wenchuan earthquake as well as stations used in this study

are generated and these phases arrive at stations at similar time with Pn under certain circumstances. Therefore, we try to use a two-layer crust model deduced from Pei et al. (2010) to recalculate the FMS of event No. 205 (a2 in Fig. 5). The recalculated FMS has only one well-constrained solution (a3 in Fig. 5), which in turn confirmed the correctness of the existence of a middle-crust interface in this region. Event No. 209 (225210320) locates near No. 205 but facing a different situation. The seismogram of nearly all the stations starts with a small and wiggling wave which is hard to distinguish. Wave generated by this event may suffer a first small creep and then a large crack. We will not include this event in the discussion of this paper, because it has large uncertainty.

Figure 4 shows the FMSs and spatial distributions of the 51 events of magnitude over 5.0 mentioned above. Well-determined FMSs are shown in red, green, and blue colors, indicating different types of events. For the poorly determined events, we plot our preferred FMSs in darker red, darker green, and darker blue. The FMSs of the 2 events that probably have biased polarities are shown in black color.

We compared our FMSs with Global CMT results as well as CAP results (Fig. 6). As shown in Fig. 6, 9 of 10 events have very similar FMSs from all three sources stated above except for the last one. No. 208 event (206070928, M_s 6.0) has very similar FMS from CMT and CAP, which is different from our result. It is a poorly constrained event with two possible FMSs with either of them feasible to explain PWFMP distribution (Fig. 7). Unfortunately, neither FMSs from CMT and CAP seems to satisfy the PWFMP distribution. This event might be averagely a strike-slip event with a thrust onset. However, it is also possible that this event might be controlled by local velocity structure similar to the case of event 205.

3.2 Characteristics of the FMSs

We obtained 129 robust FMSs for events with magnitude over M_s 4.0 in WES. All the well-determined FMSs are shown in Fig. 3 with different colors for different types of FMSs and also listed in Table 1. As shown in Fig. 3, the most abundant type of events are the red-colored ones,

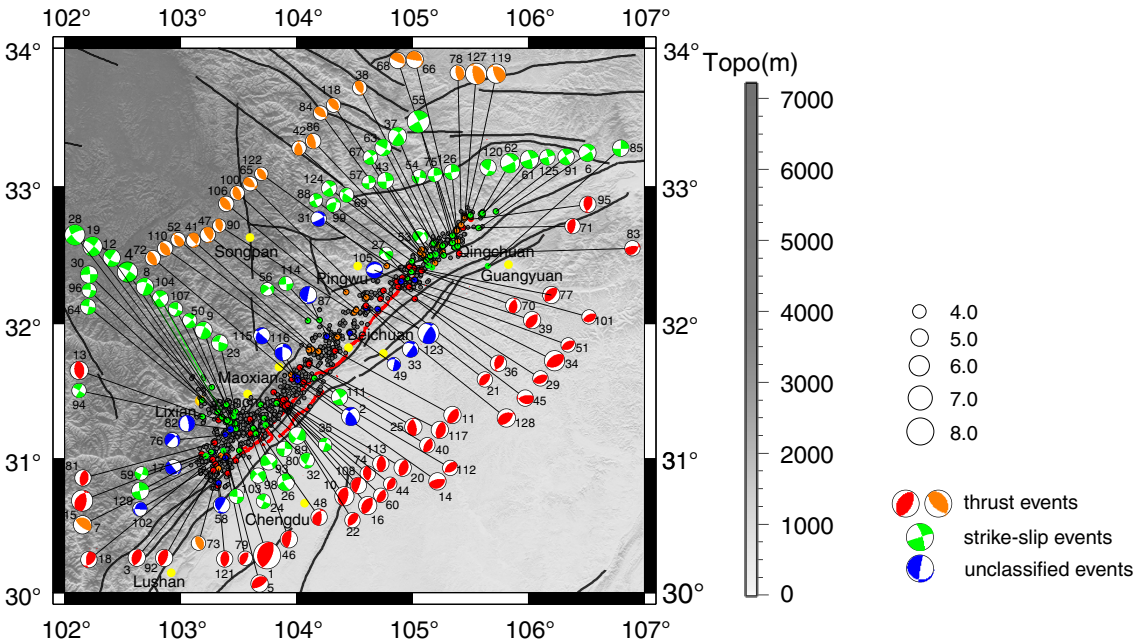

Fig. 3 Map view of the earthquake distribution and FMSs. *Base map* with *gray color*expresses the topography from ASTGTM2 (http://gdem.ersdac.jspacesystems.or.jp/). *Black dots* are relocated events between 2008.05.12 and 2008.08.01 from Cai et al. (2011). The *beach balls* with *different colors* are FMSs of different kinds. The lower hemisphere projection is adopted, of which the *quadrants filled* with *colors*are extensional quadrants and the *white ones* are compressional quadrants. The *yellow dots* are some cities in this area

totally 41, accounting for up to 30 % of all the FMSs. Similar with the main shock, they are all thrust events with their compressional directions roughly pointing NW–SE. These earthquakes were named first-type thrust events by Cai et al. (2011) and were found almost on the whole seismic belt of WES. In this paper, we further confirm the main conclusion given by Cai et al. (2011) with emphasis that they distribute unevenly.

First, the southern part of the Longmenshan fault released more elastic energy by this type of events than the northern part, which is illustrated by both source inversion results of the main shock (e.g., Ji and Hayes 2008; Shen et al. 2009) and the aftershock distribution shown in this paper.

Second, this type of events concentrate in four places along the Longmenshan fault. The first one is located at the southernmost end of the whole seismic zone. The second place is to the northeast and about 60 km away from the mainshock and locates around Maoxian. Different from the first group, the events in the second group are more tightly clustered. A vertical profile cut through this group of earthquakes in Cai et al. (2011) showed a complicated distribution of aftershocks, indicating complex faults there. These events located at the segment of the Longmenshan fault zone with two sub-parallel active faults as mentioned by Liu-Zeng et al. (2009). The third group is a small cluster near Beichuan, with only five first-type thrust events there. The northernmost group locates near the northeastern end of the surface rupture zone, 220 km away from the mainshock. However, these events in this place are more diffuse than the former three places.

Moreover, we further confirm and more clearly show that the compressional directions of the first-type thrust FMSs have systematical variation. Around Wenchuan, almost all principal compressional directions of the FMSs point roughly EW, while around Maoxian some with different principal compressional directions emerge, which roughly point to dip direction of the Longmenshan fault. To further northeast, the principal compressional directions of some FMSs of first-type thrust events even follow this trend and have larger right-lateral rotation.

Cai et al. (2011) pointed out that there is another type of thrust events existed in WES and named them second-type thrust event, which was also implied by Yi et al. (2012). Here, we further confirmed their existence (orange colored beach balls in Fig. 2). They are mostly distributed in the middle and northern segment of the Longmenshan fault zone, from Maoxian to the northeastern end of the seismic zone. The magnitude of these events is relatively small ($M_s < 4.5$) except the northeastern end (four events with $M_s \geq 5.0$). Different from Cai et al. (2011), we find two more second-type thrust events at the southwestern end of the WES and one of them is $M_s > 5.0$ event.

As shown by former results (Hu et al. 2008; Wang et al. 2009; Zheng et al. 2009, 2010; Cai et al. 2011; Yi et al. 2012), many strike-slip events with compressional directions roughly in E–W are found in WES. They mainly

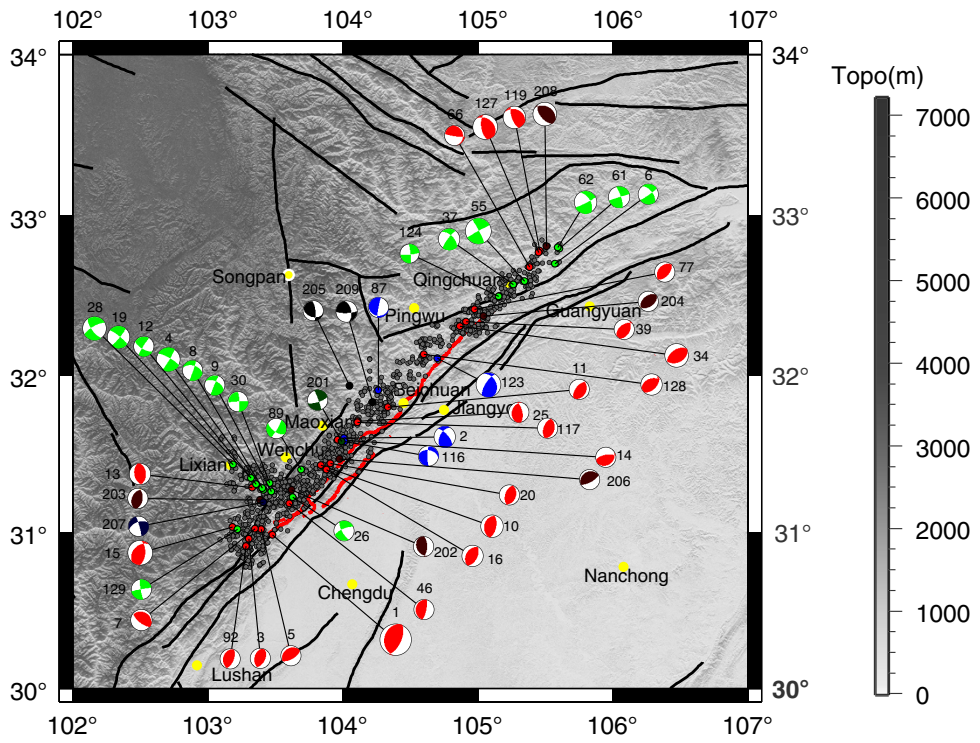

Fig. 4 Map view of the FMSs and spatial distributions of $M_s \geq 5.0$ events. *Red*, *green*, and *blue* beach balls represent different kinds of well-determined FMSs. The *serial numbers* marked beside them are the same with Fig. 3, which is aligned by the occurrence time from 1 to 129. *Dark red*, *dark green*, and *dark blue* beach balls are our preferred FMSs of the events that are not well determined due to lack of P polarity observations. *Black* beach balls are the FMSs that may have biased P polarities. The poorly determined FMSs are numerated from 201 to 209 by their occurrence time

distribute around Xiaoyudong and Hongkou area in the south and Maoxian area in the north. In Qingchuan area, almost all strike-slip events have one focal plane close to the strike of the surface rupture zone or Qingchuan fault. In Xiaoyudong-Hongkou area, about 56 % of the strike-slip events seem to occur on the left-lateral Lixian–Xiaoyudong fault with roughly NW–SE strike. Among them, most FMSs look almost the same. However, there are a few (Nos. 30, 96, and 64 in Fig. 3) that deviate a little from others.

The remaining 44 % of the strike-slip events occurred on SW–NE striking Longmenshan fault zone. Different from those on Qingchuan fault and Lixian–Xiaoyudong fault, the events on Longmenshan fault around Xiaoyudong and Hongkou area seem to be more diversified. Some FMSs (Nos. 24, 26, 32, 35, and 111) are similar with those located on Lixian-Xiaoyudong fault; however, others (Nos. 89, 80, 93, 98, and 59) are totally different. It needs to be mentioned that the second group strike-slip events on Lixian-Xiaoyudong fault can still find their companions to the north, i.e., Nos. 56, 114, 27, and 53.

Besides, there are two normal-fault events as well as some atypical events. One normal-fault event locates around Yingxiu-Hongkou (82), while another around Pingwu (105). The extensional direction of the former is E–W, while that of the latter is N–S. When we say that there are only two normal-fault events in WES, atypical events are rare too. Some of them (Nos. 2, 49, 33, 123, 115, 116, and 31) locate in the middle part of WES at about Beichuan area and look like most strike-slip events at Lixian-Xiaoyudong with little dip-slip motion. Others (Nos. 76, 17, 102, and 58) mainly locate at the southwestern end of WES around Yingxiu-Hongkou area. Most of them (Nos. 76, 17, and 102) exhibit some similarity with a group of strike-slip events occurred at Yingxiu-Hongkou area (i.e., Nos. 103, 98, 93, 80, and 89), while No. 58 looks like the ones of another group (Nos. 24, 26, 32, and 35) although it is located far away from them. Anyway, No. 87 is an exception although it has some similarity with two nearby small strike-slip events (Nos. 56 and 114) and two remote ones (Nos. 27 and 53).

4 Deductions and conjectures

4.1 Stress state deduced from the FMSs of the WES

It was often mentioned that the FMSs before and after great earthquakes are different (e.g., Xu et al. 1987, 1989; Cui et al. 2005; Yu et al. 2013). It is true that every event will produce local stress adjustment (Diao et al. 2005; Li et al. 2008). Some big events like 2011 Tohoku-Oki Earthquake

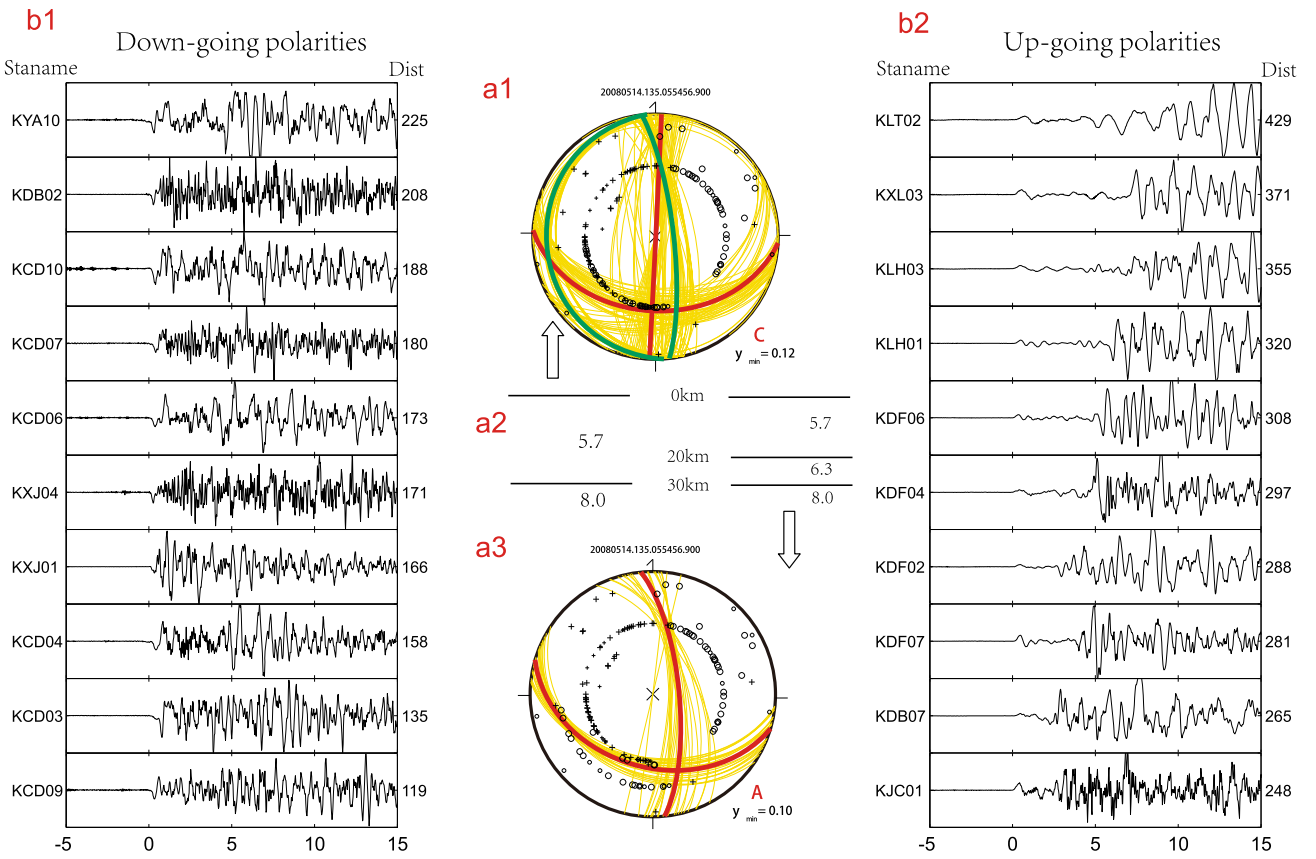

Fig. 5 FMS and waveforms of event No. 205 (135055456). **b1** and **b2** show the waveforms of down-going (epicentral distances 119–225 km) and up-going polarities (epicentral distances 248–429 km) of azimuth 180°–270°, respectively. **a1** and **a3** show the FMSs of this event with and without a crust discontinuity around 20 km depth. We could see clearly that there is only one well-constrained FMS with a two-layer crust model. **a2** The two velocity structure used for (**a1**) and (**a3**), respectively

might even change regional stress state for a long time (Yu et al. 2013). However, preexisting faults are easy to be activated and tend to prematurely release part of elastic energy stored in the lithosphere. Longmenshan region is an area highly fragmented by many faults with different strikes and dip angles. So, the FMSs of the events there might not always stand for the real regional stress. As one of the evidences, the first- and the second-type thrust events coexist on the same segment of Longmenshan fault zone, which is obviously the result controlled by the geometry of the Longmenshan faults there. These faults released different components of the elastic stress tensor as mentioned by Cai et al. (2011). Meanwhile, we mention that compared with the Yingxiu-Hongkou area, the compressional directions of the first-type thrust events located on the northeastern part of the Longmenshan fault rotate clockwise slightly, which contradicts the anti-clockwise rotation pattern of the stress field in this region. It is indeed in accordance with the clockwise rotation of the Qingchuan fault to the northeast relative to the Longmenshan fault to the southwest. In addition, the strike-slip events (Nos. 88, 124, 99, 69, 57, 67, 63, 37, 55, 43, 54, 75, 126, 120, 62, 61, 125, 91, 6, and 85) around Qingchuan area look similar but can be divided into two groups, of which one group (Nos. 57, 43, 54, 75, 126, 120, 62, 61, 125, and 85) has a nodal plane which roughly parallels to the Qingchuan fault and others (Nos. 88, 124, 99, 69, 67, 63, 37, 55, 91, and 6) have one nodal plane which roughly parallels to the strike of the Longmenshan fault. At last, events 30, 96, and 64 occurred at Lixian-Xiaoyudong fault but with a left-lateral rotation relatively to the majority of the strike-slip events there, which might also be related with one or more active faults roughly striking N–S there.

As a result, even a big event mostly could not fully express regional stress field. So, we could not directly employ either the FMS of a main shock or the ones of its aftershocks to depict the feature of a regional stress field although they partly reflect it. Only by comprehensively analyzing all FMSs in a region could we understand their geodynamical meaning and accordingly constrain regional stress state of a region semi-quantitatively. Nevertheless, if an extremely great event had released all elastic energy

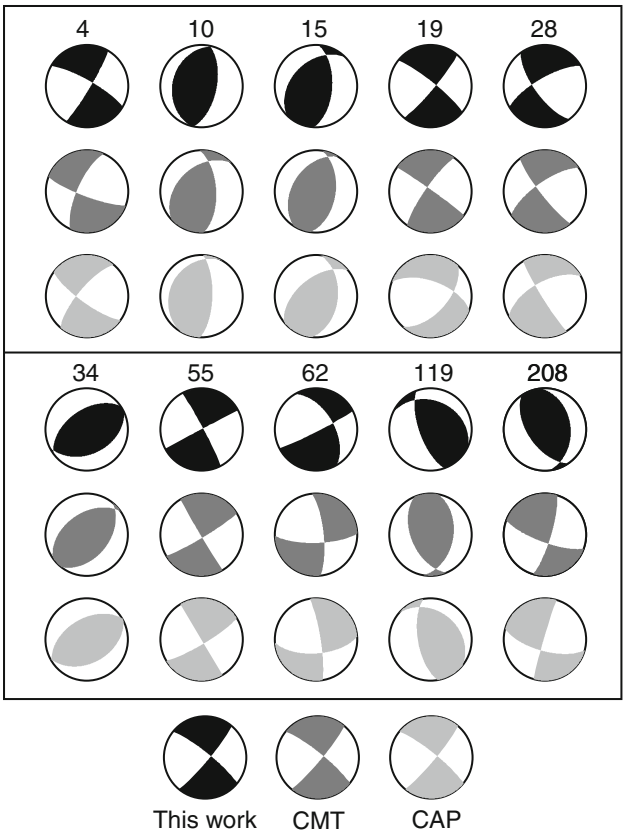

Fig. 6 Comparison among the FMSs of $M_s \geq 5.6$ events from this paper (*black*), CMT (*dark gray*, http://www.globalcmt.org/CMTsearch.html), and CAP (*light gray*, Zheng et al. 2009)

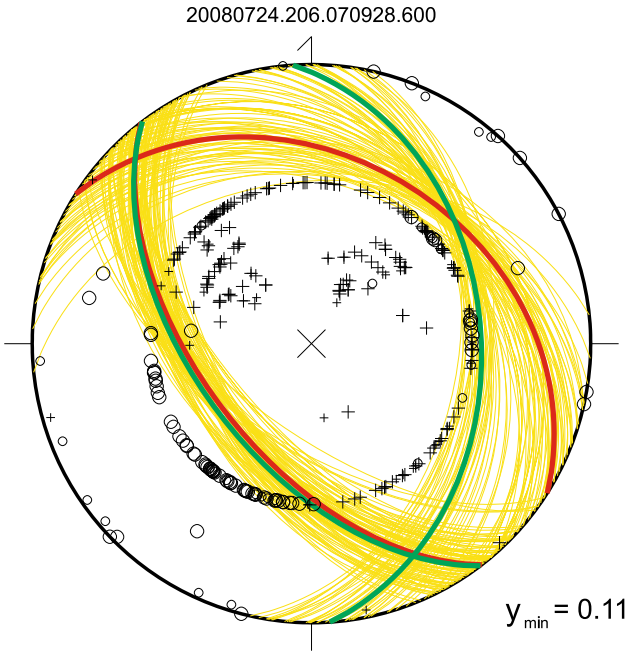

Fig. 7 The PWFMP distribution of event 208 (206070928, M_s 6.0)

stored in the competent layer of the lithosphere where it took place or occurred on a new fault, it itself might have fully expressed the interseismic regional/local stress.

Cai et al. (2011) concluded that the principal compressional direction of the regional stress is grossly perpendicular to the strike of Beichuan-Yingxiu fault around Wenchuan area. However, if we describe it more precisely, the initial rupture of the 2008 Wenchuan earthquake is almost pure reverse with the principal compressional direction pointing ESE–WNW, which is not exactly perpendicular to the strike of the Longmenshan fault but with about 10-degree left-lateral rotation. It means that the initial rupture might be newly created, not exactly along the existed fault. At the same time, The Yingxiu-Hongkou area might be nearly fully broken in the main shock, which will be discussed in Sect. 4.2.

In any case, the local principal compressional direction around Hongkou area before the 2008 Wenchuan earthquake happened should be roughly the principal compressional direction of the FMS of it, i.e., WNW–ESE. As a result, although the first-type of the thrust events distributed unevenly on the southwestern part of the WES, they were dominant there.

However, at the northeastern end (around Qingchuan) of the WES, the FMSs were obviously different. First-type thrust events belong to minority, while the strike-slip and second-type thrust events (thrust events with compressional direction roughly pointing NE–SW) dominate. Taken all events there, i.e., strike-slip events with compressional direction roughly pointing E–W, second-type thrust events with principal compressional direction roughly pointing the strike of the Longmenshan fault, as well as a few first-type thrust events with principal compressional direction roughly pointing E–W, into consideration, we reckon that the principal compressional direction of the local stress around Qingchuan was about ENE–WSW, which is similar to but slightly different from the conclusion given by Cai et al. (2011).

It is important to further mention that the compressional directions of almost all kinds of FMSs of the WES are subhorizontal (except two normal-fault events located at Hongkou and Pingwu), which is in good agreement with the conclusion given by Cai et al. (2011) but with a few corrections that the compressional directions are, respectively, WNW–ESE around Yingxiu-Hongkou and ENE–WSW around Qingchuan. We keep claiming that the gravity role of possibly existed molten material in lower crust of the Songpan-Ganze terrain seems to have minor effect on local stress state in Longmenshan region, although we still cannot deny the possible existence of molten material in the lower crust of Songpan-Garze terrain. The subhorizontal principal compressional direction along the Longmenshan Fault from SW to NE has a left-lateral rotation, which agrees well with

Table 1 The 129 well-constrained FMSs of the events with magnitudes over M_s 4.0

NUM	EVNM	LAT	LON	DEP	M_s	LOC	SK1	DA1	SA1	SK2	DA2	SA2	REL	ME
001	20080512.133.062804.000	30.986	103.479	12.9	8.0	C	190	028	077	024	062	097	1.000	P
002	20080512.133.082139.200	31.601	104.010	12.3	5.4	C	319	068	043	209	051	151	1.000	P
003	20080512.133.102339.400	30.959	103.302	20.6	5.0	C	028	050	102	190	042	076	1.000	P
004	20080512.133.111100.100	31.273	103.414	14.2	6.0	C	031	084	192	300	078	354	1.000	P
005	20080512.133.134053.400	31.020	103.394	14.6	5.2	C	231	026	081	061	064	094	1.000	P
006	20080512.133.144608.600	32.701	105.572	21.0	5.1	C	055	084	212	322	058	353	1.000	P
007	20080512.133.152852.300	31.024	103.351	17.8	5.3	C	128	068	094	297	022	081	1.000	P
008	20080512.133.172904.400	31.282	103.403	13.5	5.1	C	019	086	222	286	048	355	1.000	P
009	20080512.133.175430.800	31.259	103.469	11.1	5.0	C	296	054	006	203	085	143	1.000	P
010	20080512.133.200848.500	31.428	103.837	12.8	5.6	C	194	030	092	011	060	089	1.000	P
011	20080512.133.204530.800	31.795	104.335	09.8	5.0	C	218	057	098	024	033	078	1.000	P
012	20080512.133.234617.300	31.307	103.358	14.1	5.0	C	212	084	202	120	068	354	1.000	P
013	20080512.133.235445.400	31.287	103.328	13.4	5.4	C	169	047	084	358	044	096	1.000	P
014	20080513.134.021516.600	31.588	103.962	25.8	5.0	C	259	066	101	054	026	067	1.000	P
015	20080513.134.070707.200	31.035	103.184	13.6	6.1	C	225	040	124	003	058	065	0.682	AR
016	20080513.134.082050.500	31.400	103.879	04.8	5.3	C	213	036	095	027	054	087	1.000	P
017	20080513.134.193016.100	31.051	103.278	16.7	4.7	C	052	019	000	322	090	109	0.981	AR
018	20080513.134.195152.300	30.996	103.280	14.6	4.8	C	181	058	057	051	044	131	1.000	P
019	20080514.135.025435.500	31.348	103.320	07.1	5.6	C	040	083	189	309	081	353	1.000	P
020	20080514.135.092643.300	31.440	103.910	15.5	5.0	W	198	052	090	017	038	089	1.000	P
021	20080514.135.104436.700	32.179	104.727	09.1	4.4	C	227	038	097	038	052	084	1.000	P
022	20080514.135.171721.800	31.495	103.806	20.3	4.5	C	204	039	074	044	053	102	1.000	P
023	20080514.135.173322.300	31.349	103.476	21.6	4.7	C	189	076	169	282	079	014	1.000	P
024	20080514.135.195900.900	31.059	103.508	10.8	4.3	C	023	087	−178	293	088	−03	1.000	P
025	20080514.135.210105.800	31.707	104.109	08.4	5.1	C	197	030	115	349	063	077	0.818	AR
026	20080514.135.221008.800	31.227	103.630	20.1	5.0	C	247	072	199	151	072	341	1.000	P
027	20080515.136.125412.000	32.328	104.956	20.8	4.0	C	152	074	155	250	066	018	1.000	P
028	20080516.137.052546.300	31.432	103.187	06.8	5.9	C	240	073	201	144	070	342	1.000	P
029	20080516.137.201521.000	32.268	104.874	11.0	4.5	C	250	054	091	068	036	088	1.000	P
030	20080516.137.201650.400	31.314	103.460	02.1	5.0	C	358	081	184	267	086	351	1.000	P
031	20080516.137.223308.300	32.318	105.021	11.7	4.4	C	062	081	238	318	033	343	1.000	P
032	20080516.137.232306.500	31.299	103.721	23.4	4.5	C	026	079	143	124	054	014	1.000	P
033	20080517.138.133212.600	32.113	104.605	19.3	4.7	C	217	088	126	310	036	004	1.000	P
034	20080517.138.170824.800	32.308	104.868	20.5	6.0	C	235	050	084	064	040	097	1.000	P
035	20080518.139.125240.600	31.412	103.828	25.1	4.0	C	021	090	207	291	063	360	1.000	P
036	20080519.140.040857.800	32.180	105.020	19.0	4.7	Q	183	047	061	041	050	117	1.000	P
037	20080519.140.060652.500	32.567	105.263	17.4	5.4	C	217	078	147	314	058	014	1.000	P
038	20080519.140.062549.900	32.520	105.262	19.0	4.2	C	141	054	064	001	043	121	1.000	P
039	20080519.140.175233.100	32.335	104.914	22.1	5.0	C	233	047	109	026	046	071	1.000	P
040	20080520.141.005736.200	31.676	104.027	17.9	4.4	C	208	060	092	024	030	087	1.000	P
041	20080520.141.065420.900	31.794	104.192	07.3	4.3	C	136	079	057	030	035	161	1.000	P
042	20080520.141.142940.800	32.502	105.090	23.8	4.3	C	206	042	128	340	058	061	1.000	P
043	20080521.142.093315.200	32.462	105.121	02.5	4.6	C	237	085	161	329	071	005	1.000	P
044	20080521.142.135906.300	31.419	103.885	17.0	4.5	C	168	035	076	005	056	100	1.000	P
045	20080521.142.203627.000	32.240	104.750	15.2	4.8	W	257	062	069	116	034	124	0.805	AR
046	20080522.143.071842.900	31.185	103.606	07.4	5.1	C	185	015	083	013	075	092	0.865	AR
047	20080522.143.150012.700	31.900	104.354	08.6	4.6	C	145	070	064	020	032	141	1.000	P
048	20080522.143.173736.800	31.292	103.600	15.1	4.9	C	232	035	136	360	067	063	1.000	P

Table 1 continued

NUM	EVNM	LAT	LON	DEP	M_s	LOC	SK1	DA1	SA1	SK2	DA2	SA2	REL	ME
049	20080522.143.195849.400	31.927	104.461	11.9	4.0	C	011	089	244	278	026	358	1.000	P
050	20080523.144.012328.100	31.220	103.480	14.4	4.3	W	044	079	205	309	066	347	1.000	P
051	20080523.144.161022.800	32.267	104.969	11.3	4.3	C	238	048	088	060	042	092	1.000	P
052	20080523.144.164803.900	31.808	104.133	18.6	4.3	C	305	052	062	166	046	121	1.000	P
053	20080523.144.175332.600	32.504	105.199	13.0	4.4	C	041	087	049	307	041	176	1.000	P
054	20080524.145.114213.400	32.558	105.366	13.6	4.1	C	102	087	−175	012	085	−03	1.000	P
055	20080525.146.082149.300	32.590	105.345	26.6	6.4	C	242	089	176	332	086	001	1.000	P
056	20080525.146.182053.500	32.020	104.100	02.0	4.0	Q	314	062	175	046	085	028	1.000	P
057	20080525.146.234719.600	32.423	105.136	17.7	4.1	C	302	084	041	207	049	172	1.000	P
058	20080526.147.003947.500	30.819	103.328	17.9	4.8	C	135	027	015	031	083	116	0.797	AR
059	20080526.147.230126.200	31.051	103.267	19.4	4.0	C	110	079	187	018	083	349	1.000	P
060	20080526.147.232204.600	31.397	103.899	24.0	4.2	C	215	061	099	016	031	074	1.000	P
061	20080527.148.080322.500	32.795	105.605	19.6	5.4	C	252	089	168	343	078	001	1.000	P
062	20080527.148.083751.300	32.800	105.591	18.0	5.7	C	330	054	355	062	086	216	1.000	P
063	20080527.148.135933.500	32.588	105.184	05.9	4.9	C	025	059	177	117	087	031	1.000	P
064	20080527.148.141400.300	31.273	103.427	19.7	4.5	C	010	086	−177	280	087	−04	1.000	P
065	20080527.148.164606.700	32.192	104.606	15.8	4.3	C	331	053	128	099	051	051	1.000	P
066	20080527.148.173508.600	32.679	105.384	22.6	5.0	C	098	083	071	347	020	158	1.000	P
067	20080528.149.174710.400	32.498	105.271	10.9	4.3	C	238	085	158	330	068	006	1.000	P
068	20080529.150.044844.500	32.600	105.390	14.9	4.7	C	113	078	078	340	017	136	1.000	P
069	20080529.150.204007.500	32.410	105.170	12.6	4.0	W	086	079	183	355	087	349	1.000	P
070	20080531.152.062241.200	32.404	105.014	23.3	4.4	C	213	046	119	354	051	063	1.000	P
071	20080531.152.073422.100	32.698	105.439	19.8	4.4	C	186	026	084	012	064	093	0.688	AR
072	20080601.153.032357.800	31.622	103.956	21.5	4.5	C	150	029	087	333	061	092	1.000	P
073	20080604.156.081940.800	30.928	103.330	11.1	4.3	C	158	059	089	341	032	092	0.458	AR
074	20080604.156.112346.600	31.437	103.888	15.8	4.0	C	206	057	084	036	033	099	1.000	P
075	20080604.156.114508.500	32.641	105.345	18.6	4.2	C	082	081	167	174	077	010	1.000	P
076	20080604.156.212139.000	31.178	103.386	19.9	4.5	C	330	033	197	226	081	302	1.000	P
077	20080605.157.044106.400	32.414	104.974	18.6	5.1	C	221	035	089	042	055	091	1.000	P
078	20080605.157.060228.600	32.722	105.422	12.0	4.6	C	172	065	100	330	027	071	1.000	P
079	20080605.157.063526.100	30.890	103.407	14.3	4.1	C	218	025	102	025	065	085	1.000	P
080	20080606.158.110349.000	31.251	103.733	21.9	4.4	C	274	086	176	004	086	004	0.275	AR
081	20080606.158.143846.200	31.116	103.297	22.1	4.7	C	189	055	086	016	035	095	1.000	P
082	20080607.159.004810.000	31.218	103.431	17.4	4.8	C	352	072	−96	191	019	−72	1.000	P
083	20080607.159.062832.500	32.513	105.405	17.6	4.5	C	033	036	043	266	066	118	1.000	P
084	20080607.159.073245.600	32.539	105.080	02.0	4.3	C	331	040	119	114	056	068	0.539	AR
085	20080607.159.104203.800	32.420	105.650	19.0	4.8	Q	090	086	178	180	089	004	1.000	P
086	20080607.159.221429.500	32.516	105.068	07.3	4.6	C	158	019	084	344	071	092	1.000	P
087	20080608.160.105116.800	31.904	104.264	03.6	5.1	C	093	019	352	191	087	251	1.000	P
088	20080608.160.225537.100	32.379	104.992	05.9	4.0	C	251	083	−167	160	077	−07	1.000	P
089	20080609.161.072836.800	31.400	103.690	22.6	5.0	C	125	064	189	031	082	334	1.000	P
090	20080609.161.232013.600	32.082	104.499	14.0	4.0	C	155	049	072	001	044	109	0.457	AR
091	20080610.162.162727.500	32.820	105.720	33.0	4.8	Q	237	081	180	147	090	351	1.000	P
092	20080610.162.222318.600	30.913	103.282	16.4	5.0	C	192	030	081	022	060	095	1.000	P
093	20080615.167.001121.700	31.185	103.651	15.4	4.9	C	329	079	156	064	066	012	1.000	P
094	20080615.167.214239.000	31.310	103.191	25.8	4.1	C	029	087	−179	299	089	−03	0.914	AR
095	20080617.169.055141.900	32.762	105.503	02.5	4.7	C	027	050	116	169	047	062	1.000	P
096	20080617.169.224313.000	31.287	103.394	12.2	4.2	C	007	071	−173	275	084	−20	1.000	P

Table 1 continued

NUM	EVNM	LAT	LON	DEP	M_s	LOC	SK1	DA1	SA1	SK2	DA2	SA2	REL	ME
097	20080618.170.125931.900	29.150	102.280	14.0	4.8	Q	092	086	175	182	085	004	1.000	P
098	20080619.171.025528.600	31.220	103.432	17.4	4.6	C	322	085	201	230	069	354	1.000	P
099	20080621.173.040304.400	32.457	104.996	22.6	4.2	C	256	061	144	005	059	034	1.000	P
100	20080622.174.103734.200	32.230	104.430	17.0	4.3	Q	165	035	095	339	055	086	0.895	AR
101	20080622.174.213831.300	32.384	105.081	19.5	4.1	C	244	057	087	069	033	095	0.764	AR
102	20080623.175.181837.400	31.007	103.388	10.7	4.1	C	094	086	117	191	028	009	1.000	P
103	20080627.179.005541.700	31.060	103.373	04.6	4.3	C	001	082	176	091	086	008	1.000	P
104	20080627.179.182053.500	31.530	103.270	01.0	4.8	Q	235	078	185	144	085	348	1.000	P
105	20080627.179.214211.800	32.307	104.906	20.2	4.8	C	085	058	−87	259	032	−95	1.000	P
106	20080628.180.235520.400	32.099	104.516	16.5	4.6	C	132	038	076	330	053	100	1.000	P
107	20080629.181.195137.500	31.400	103.396	05.0	4.1	C	017	068	179	108	089	022	1.000	P
108	20080701.183.195753.100	31.388	103.903	22.2	4.8	C	162	014	054	019	079	098	1.000	P
109	20080702.184.235106.900	27.398	102.713	12.1	4.1	C	258	089	163	348	073	001	1.000	P
110	20080704.186.221053.700	31.802	104.110	18.7	4.6	C	147	036	091	326	054	089	1.000	P
111	20080705.187.070045.300	31.598	104.153	12.4	4.7	C	060	075	183	329	087	345	1.000	P
112	20080705.187.185013.000	31.570	104.062	16.0	4.5	C	222	047	074	065	046	106	1.000	P
113	20080708.190.121257.500	31.400	103.926	22.6	4.9	C	188	048	096	359	042	083	1.000	P
114	20080710.192.193602.100	32.023	104.200	00.8	4.2	C	355	088	174	085	084	002	1.000	P
115	20080714.196.195633.100	31.612	103.988	13.2	4.8	C	311	086	057	216	033	174	1.000	P
116	20080715.197.092620.500	31.578	104.013	12.3	5.0	C	180	079	308	284	040	197	1.000	P
117	20080717.199.164041.100	31.701	104.110	28.2	5.1	C	200	054	094	013	037	085	1.000	P
118	20080718.200.012601.800	32.441	105.195	16.2	4.3	C	132	058	077	336	035	110	0.979	AR
119	20080723.205.195443.700	32.782	105.460	08.6	5.6	C	160	068	111	295	030	049	1.000	P
120	20080724.206.053009.000	32.792	105.501	08.7	4.8	C	019	075	154	116	065	017	1.000	P
121	20080724.206.205415.100	30.797	103.324	15.7	4.7	C	180	046	083	010	044	097	0.626	AR
122	20080729.211.220329.300	32.420	104.780	18.0	4.0	Q	324	045	089	146	045	091	1.000	P
123	20080801.214.083242.300	32.104	104.699	19.2	6.1	C	212	069	119	334	035	038	1.000	P
124	20080801.214.181216.700	32.494	105.156	21.0	4.8	C	084	083	185	353	085	353	1.000	P
125	20080802.215.132545.900	32.806	105.606	19.3	4.6	C	255	087	176	345	086	003	1.000	P
126	20080802.215.133559.600	32.567	105.394	23.0	4.5	C	083	085	168	174	078	005	1.000	P
127	20080805.218.094915.600	32.770	105.450	16.0	6.2	Q	171	063	110	312	033	057	1.000	P
128	20080807.220.081534.300	32.130	104.600	24.0	5.3	Q	252	041	112	044	052	072	1.000	P
129	20080814.227.170638.500	31.020	103.220	18.0	5.1	Q	260	087	186	170	084	357	1.000	P

NUM the number of each event, which is the same as shown in Figs. 3 and 4, *EVNM* event name, *LAT* latitude, *LON* longitude, *DEP* depth, M_s surface wave magnitude, *LOC* sources of spatial distributions (*C* Cai et al. 2011, *W* Wu et al. 2009, *Q* quick location from CEA), *SK1*, *DA1*, and *SA1* are, respectively, the strike, dip angle, and slip angle of the first focal plane, *SK2*, *DA2*, and *SA2* are those of the second focal plane, *REL* reliability of P-wave first-motion solution (the number shows how many cluster centers of possible solutions), *ME* methods used when determining the solution (*P* only PWFMP is used, *AR* both PWFMP and AR are used)

former predictions for regional stress field (e.g., Xu et al. 1987, 1989; Cui et al. 2005). The controlling power of the stress field in this region should be the eastward horizontal push from Tibetan plateau.

In April 20, 2013, an M_w 6.7 earthquake attacked the Lushan town of Yaan city to the southwest of Wenchuan. The focal mechanism solution of this event shows that this is a pure thrust event with the compressional direction roughly NW–SE (Zhang et al. 2013), which is almost exactly perpendicular to the strike of the Longmenshan fault there. Meanwhile, the FMSs of its aftershocks are mostly thrust-type events that are similar to the main shock (Lv et al. 2013). Furthermore, the rupture process and spatial distribution of its aftershocks do not show a predominant direction similar to WES. This result further confirms our judgment on variation pattern of the regional stress around Longmenshan fault region.

4.2 Broken barriers and ready-to-be-broken barrier

There were diversity of the FMSs and less seismicity after the 2008 Wenchuan earthquake in the intermediate part of

the Longmenshan fault around Gaochuan-Beichuan area. Cai et al. (2011) claimed that small elastic energy accumulation in there might be an explanation when they noticed a triangle region inside the Songpan-Garze terrain around Gaochuan-Beichuan area. As the lithosphere of the Tibetan Plateau faces great resistance from Sichuan Block, it tends to move toward southeast (Chuandian block direction) and northeast (Qinling direction). Similarly, the northern and southern parts of the Songpan-Garze block move more quickly compared with its central part, which leads to small push acting on Gaochuan-Beichuan area. For similar reason, although the motion at Yingxiu-Hongkou might have triggering role on the motion at Beichuan-Qingchuan when the 2008 Wenchuan earthquake was initiated at Yingxiu-Hongkou and later propagated to northeast, the strike-slip motion at Beichuan or to its northeast might be mainly pushed by intensified drag force from far west after Yingxiu-Hongkou lost its competence, which was mentioned in Sect. 4.1 and will be explained in more detail below. A short pause between the motions of the two regions and intensity variation of the rupture along the Longmenshan fault during the 2008 Wenchuan earthquake, as well as great aftershock activity around Maoxian, are all manifestations for more complex triggering role.

However, after realizing that the great energy released around Gaochuan-Beichuan in the main shock (e.g., Ji and Hayes 2008; Zhang et al. 2009; Shen et al. 2009; Wang et al. 2011) and some aftershocks which might stand for releasing of the local elastic energy produced by the strike-slip motion around Beichuan in the main shock, we have to adjust our understanding and claim that low seismicity and diversity of the FMSs around Beichuan area after the main shock might be mainly the results of nearly fully energy releasing of it in the main shock although we still think that there is relatively less elastic energy accumulation in the middle part of the Longmenshan fault, keeping the judge that there is less risk of great earthquakes in the near future around there.

Similarly, there were only a few big events of the same kind occurred around Yingxiu-Hongkou. Among them, the ones to the northeast of the main shock were more sporadic. Moreover, there were also some events at Yingxiu area with nearly E–W principal extensional direction (Nos. 17, 76, and 82). One of them was even normal (No. 82). So, the Yingxiu area of about 800 km^2 in its size might have been nearly thoroughly destroyed by the 2008 Wenchuan earthquake. The main shock might be initiated at nearly the southwest end of the 800 km^2 area and then propagated northeastward along the Longmenshan fault. At last, it thoroughly broke the Yingxiu area in one action and produced maximum dislocation there as shown by source rupture inversions (e.g., Ji and Hayes 2008; Zhang et al. 2009).

In Sect. 4.1, we stated the possibility that the Yingxiu-Hongkou and Beichuan might be nearly fully broken. In contrast, all evidences from the 2008 Wenchuan earthquake (e.g., Zhang et al. 2009; Liu-Zeng et al. 2009) and its aftershocks (both spatial distribution and FMSs) seem to imply that the main shock had less extension to southwest direction along the Longmenshan fault. In other words, its motion dramatically decreased southwestward. This judgement not only further supports that the compressional direction of the stress field before the 2008 Wenchuan earthquake around Yingxiu-Hongkou was skewed with the strike of the Longmenshan fault, but also implies that the region to the southwest of Yingxiu-Hongkou did not release as much energy as the area to the northeast of it.

Although there is a tiny possibility that the elastic energy to the southwest of Yingxiu-Hongkou had already been released by one or more big historical events before, we have a few evidences which weakly say that a big barrier might exist to the southwest of Hongkou although we do not know how strong it is and how much elastic energy has already been accumulated in it since last break. First, many first-type thrust events of the WES in Hongkou area only occurred near the southwestern end of the 800 km^2 broken area but with no further penetration southwestward, leaving a big blank there. In the Longmenshan area, it is difficult to think that there is no elastic energy accumulation after years of quiescence. Second, there are no FMSs with extensional direction roughly pointing E–W outside the fully broken area to the southwest of Hongkou, let alone normal FMSs. Third, as mentioned above, the 2013 Yaan earthquake was driven by the same regional stress field and still did not disturb the quiescence of that blank area. Fourth, some transitional events occurred at the southwest boundary of the fully broken area (atypical events: 17 and 102; thrust events: 7 and 73; strike-slip event 103), which were regularly distributed and might be adjustments to the 2008 Wenchuan earthquake as explained below.

4.3 Triggering role of some biggest events of WES on others

For releasing the elastic energy produced by the 2008 Wenchuan earthquake at the northern end of Yingxiu-Hongkou area, a series of strike-slip events were triggered on the Lixian-Xiaoyudong fault (Nos. 23, 9, 50, 8, 4, 12, 19, 28, 30, and 64). Events 94, 96, 104, and 107 are a little bit far away from the broken area around Yingxiu-Hongkou and might also be triggered by the main shock but mainly via inelastic process.

Some other strike-slip events, which seemed to take place on the Longmenshan fault (24, 26, 32, and 35), might play similar role if the nodal planes which are perpendicular to the strike of Longmenshan fault are the true fault planes. Certainly, it is also possible or even most probable that they might occur on the fault planes which are roughly

parallel to the Longmenshan fault belt for releasing the shear energy unreleased in the main shock.

Another group of events which played similar role but at the southern end of the Yingxiu-Hongkou area are 59, 102, and 129, of which both the numbers and the magnitudes are much smaller than those on Lixian-Xiaoyudong fault at the northern end, which further implies that the thrust motion in Yingxiu-Hongkou is asymmetrical.

Similarly, events 111, 115, and 116, low quality event 201 either, might occur for absorbing the elastic energy produced by the thrust events occurred around Maoxian if the nodal planes which are perpendicular to the strike of Longmenshan fault are the true fault planes. However, it is more possible that they might occur only or simultaneously for releasing the shear energy unreleased in the main shock. Events 89 and 81 might do only for the thrust events occurred around Maoxian but at the opposite side. Events 93, 98, also the low quality event 207, are a little bit far away from Maoxian. So, it is difficult for them to play the role similar to events 94, 96, 104, and 107 because the thrust events around Maoxian are too small and the energy accumulated by them cannot compare with the main shock. However, when mentioning that 6 of 11 aftershocks happened in the first 3 hours after the 2008 Wenchuan Event with no FMSs are just located around Yingxiu-Hongkou area, we should realize that events 93, 98, and 207 were most probably for releasing the elastic energy locally produced by some of them but mainly via inelastic processes, so do events 32 and 35 to the opposite side but triggered more elastically by those 6 events.

Events 27, 53, 56, 87, and 114, low quality event 205 either, which located around Beichuan, might play similar role as well but might mainly for right-lateral strike-slip motion of the Longmenshan fault at Beichuan where was the second place of maximum energy releasing of the 2008 Wenchuan earthquake (e.g., Ji and Hayes 2008; Wang et al. 2009; Liu-Zeng et al. 2009; Shen et al. 2009). So did events 49, 33, 123, 2, 111, 115, 116, and 201 but to the opposite site of Beichuan although 115, 116, and 201 might have been triggered mainly by the thrust events around Maoxian. However, events 49, 33, and 133 should be mainly for releasing the remaining energy unreleased by the main shock around Beichuan. By all means, above differences as well as existence of the second-type thrust events clearly depict that the material between Qingchuan fault and Beichuan fault has moved northeastward relative to its surrounding blocks although the strike-slip events around Qingchuan are mainly dextral.

5 Conclusions

P-wave first-motion polarity (PWFMP) is well-defined signal which suffers little influence from mechanical properties of the media. With enough high quality polarity data, one may obtain the FMSs with enough confidence. Yu et al. (2009) refined the method and showed a new grid search program of calculating P-wave first-motion FMSs. Compared to former grid search programs, CHNTYX has better performance on those events with sparse or unevenly distributed P-wave first-motion observations. However, while Yu et al. (2009) showed that at least one cluster of possible solutions of an event should be very close to the true solution, the new method still needs more knowledge to determine which one is right when there are several choices. Here, we employ AR of SH-wave to P-wave to help us evaluate which cluster is closest to its true FMS. Instead of taking AR observations into inversion, we plot SH/P ratio observations of an event on a colored beach ball with its colors representing theoretical ratios, and then pick out a correct cluster manually from those possible solutions given by CHNTYX. In this way, AR ratio data perfectly serve as complement to the PWFMP data, assuring both high quality and more FMSs. Totally, 129 events with magnitude over M_s 4.0 in WES are identified to be well-constrained and unique FMSs. Moreover, for comprehensively understanding the stress field in this region, we also analyze all poorly constrained events with magnitude over 5.0.

Our results reconfirm that the compressional directions of most FMSs of the WES are subhorizontal, which is in good agreement with the conclusion given by Cai et al. (2011) but with a few corrections that the compressional directions are, respectively, WNW–ESE around Yingxiu-Hongkou and ENE–WSW around Qingchuan. It seems that the subhorizontal compressional direction along Longmenshan fault has a left-lateral rotation, which agrees well with former predictions (e.g., Xu et al. 1987, 1989; Cui et al. 2005). The controlling power of the stress field in this region should be the eastward horizontal pushing from Tibetan plateau. So, we keep claiming that the gravity role of possibly existed molten material in lower crust of the Songpan-Garze terrain seems to have minor influence on local stress state in Longmenshan region, although we still cannot deny the possible existence of molten material in the lower crust of Songpan-Ganze terrain.

However, since faults are weak and easy to be broken, the earthquakes are easy to occur on them with FMSs different from regional stress field. Thrust events with perpendicular compressional directions coexist on the same segment of Longmenshan fault zone, which is obviously the result controlled by the geometry of the Longmenshan faults there. Meanwhile, compared with the Yingxiu-Hongkou area, the compressional directions of the first-type thrust events located on the northeastern part of the Longmenshan fault rotate clockwise slightly, which

contradicts the anti-clockwise rotation pattern of the stress field in this region. It is indeed in accordance with the clockwise rotation of the Qingchuan fault to the north relative to the Longmenshan fault to the south. In addition, the strike-slip events around Qingchuan area look similar but can be divided into two groups, of which one group has one nodal plane roughly parallel to the Qingchuan fault and others have one nodal plane roughly parallel to the strike of the Longmenshan fault.

At the same time, some aftershocks of the 2008 Wenchuan earthquake seem to occur just for releasing the elastic energy produced by the 2008 Wenchuan earthquake and some of its strong aftershocks. For example, a series of strike-slip events were triggered on Lixian-Xiaoyudong fault possibly for releasing the elastic energy produced by the 2008 Wenchuan earthquake at the northern end of Yingxiu-Hongkou area. Some events are a little bit far away from the broken area around Yingxiu-Hongkou and might also be triggered by the main shock but likely mainly via inelastic process. On the southern end of Yingxiu-Hongkou area, there are another group of events playing similar role although both the number and their magnitudes are much smaller than those on Lixian-Xiaoyudong fault at the northern end.

Moreover, our results clearly show that the Yingxiu-Hongkou area was nearly fully destroyed by the 2008 Wenchuan earthquake, while Beichuan is another place where accumulated energy might be nearly fully released. Low seismicity and diversity of the FMSs after the main shock around both Yingxiu-Hongkou and Beichuan might be mainly the results of nearly fully energy releasing by the main shock although we still think that relatively less elastic energy accumulation in the middle part of the Longmenshan fault is another reason for low seismicity around Beichuan. Contrarily, we propose that there might indeed exist a big barrier to the southwest of Yingxiu-Hongkou and need to pay attention on it in the near future.

Acknowledgments Thanks are given to two anonymous reviewers for helpful suggestions. Waveform data for this study are mainly provided by Data Management Center of China National Seismic Network at Institute of Geophysics, China Earthquake Administration. Profess Qiyuan Liu and Jiuhui Chen of Institute of Geology, China Earthquake Administration provided us some wave form data recorded by their Western Sichuan Passive Seismic Arrays (WSPSA). This work was supported by the Wenchuan Fault Scientific Drilling Program (WFSD). We would like to acknowledge all the people who helped us in completion of this paper.

References

Brillinger DR, Udias A, Bolt BA (1980) A probability model for reginal focal mechanism solutions. Bull Seismol Soc Am 70(1):149–170

Burchfiel BC, Royden LH, Van der Hilst RD, Hager BH (2008) A geological and geophysical context for the Wenchuan earthquake of 12 May 2008, Sichuan, People's Republic of China. GSA Today 18:4–11

Cai C, Yu CQ, Tao K, Hu XP, Tian Y, Zhang H, Cui XF, Ning JY (2011) Spatial distribution and focal mechanism solutions of the Wenchuan earthquake series: Results and implications. Earthq Sci 24(1):115–125

Cui XF, Xie FR, Zhao JT (2005) The regional characteristics of focal mechanism solutions in China and adjacent areas. Seismol Geol 27(2):234–242

Diao GL, Wang HT, Gao GY, Long HY, Nie XH (2005) A deflection process for stress field of the Jiashi strong earthquake sequence. Chin J Geophys 48(5):1062–1068

Hardebeck JL, Shearer PM (2002) A new method for determining first-motion focal mechanisms. Bull Seismol Soc Am 92(6): 2264–2276

Hardebeck JL, Shearer PM (2003) Using S/P amplitude ratios to constrain the focal mechanisms of small earthquakes. Bull Seismol Soc Am 93(6):2434–2444

Hu XP, Yu CQ, Tao K, Cui XF, Ning JY (2008) Focal mechanism solutions of Wenchuan earthquake and its strong aftershocks obtained from initial P wave polarity analysis. Chin J Geophys 51(6):1711–1718

Ji C, Hayes G (2008) Preliminary result of the May 12, 2008 M_W7.9 eastern Sichuan, China earthquake. US Geological Survey, Reston

Kasahara K (1963) Computer program for a fault-plane solution. Bull Seismol Soc Am 53(1):1–13

Kisslinger C (1980) Evaluation of S to P amplitude ratios determining focal mechanisms from regional network observations. Bull Seismol Soc Am 70(4):999–1014

Kisslinger C, Bowman JR, Koch K (1981) Procedures for computing focal mechanisms from local (SV/P)z data. Bull Seismol Soc Am 71(6):1719–1729

Li RS, Cui XF, Diao GL, Zhang HY (2008) Temporal and spatial variation of the present crustal stress in northern part of North China. Acta Seismol Sin 30(6):570–580

Lin AM, Ren ZK, Jia D, Wu XJ (2009) Co-seismic thrusting rupture and slip distribution produced by the 2008 M_W7.9 Wenchuan earthquake, China. Tectonophysics 471(3–4):203–215

Liu Q-Y, Chen J-H, Li S-C, Li Y, Guo B, Wang J, Qi S (2008) The M_S8.0 Wenchuan Earthquake: preliminary results from the western Sichuan mobile seismic array observations. Seismol Geol 30(3):584–596

Liu-Zeng J, Zhang Z, Wen L, Tapponnier P, Sun J, Xing X, Hu G, Xu Q, Zeng L, Ding L, Ji C, Hudnut KW, van der Woerd J (2009) Co-seismic ruptures of the 12 May 2008, M_S8.0 Wenchuan earthquake, Sichuan: East–west crustal shortening on oblique, parallel thrusts along the eastern edge of Tibet. Earth Planet Sci Lett 286(3–4):355–370

Liu-Zeng J, Wen L, Sun J, Zhang Z, Hu G, Xing X, Zeng L, Xu Q (2010) Surficial slip and rupture geometry on the Beichuan fault near Hongkou during the M_W7.9 Wenchuan Earthquake, China. Bull Seismol Soc Am 100(5):2615–2650

Loveless JP, Meade BJ (2011) Partitioning of localized and diffuse deformation in the Tibetan Plateau from joint inversions of geologic and geodetic observations. Earth Planet Sci Lett 303(1–2):11–24

Lv J, Wang XS, Su JR, Pan LS, Li Z, Yin LW, Zeng XF, Deng H (2013) Hypocentral location and source mechanism of the M_S7.0 Lushan earthquake sequence. Chin J Geophys 56(5):1753–1763

Meade BJ (2007) Present-day kinematics at the India-Asia collision zone. Geology 35(1):81–84

Nakamura A, Horiuchi S, Hasegawa A (1999) Joint focal mechanism determination with source-region station corrections using short-

period body-wave amplitude data. Bull Seismol Soc Am 89(2):373–383

Nakamura T, Tsuboi S, Kaneda Y, Yamanaka Y (2010) Rupture process of the 2008 Wenchuan, China earthquake inferred from teleseismic waveform inversion and forward modeling of broadband seismic waves. Tectonophysics 491(1–4):72–84

Pei SP, Su JR, Zhang HJ, Sun YS, Toksöz MN, Wang Z, Gao X, Liu-Zeng J, He JK (2010) Three-dimensional seismic velocity structure across the 2008 Wenchuan M_S8.0 earthquake, Sichuan, China. Tectonophysics 491(1–4):211–217

Rau R-J, Wu FT, Shin T-C (1996) Regional network focal mechanism determination using 3D velocity model and SH/P amplitude ratio. Bull Seismol Soc Am 86(5):1270–1283

Reasenberg P, Oppenheimer D (1985) FPFIT, FPPLOT, and FPPAGE: FORTRAN computer programs for calculating and displaying earthquake fault-plane solutions. U.S. Geological Survey, Open File Report 85-739, 109 pp

Shen Z-K, Sun JB, Zhang PZ, Wan YG, Wang M, Burgmann R, Zeng YH, Gan WJ, Liao H, Wang QL (2009) Slip maxima at fault junctions and rupturing of barriers during the 2008 Wenchuan earthquake. Nat Geosci 2(10):718–724

Wang QC, Chen ZL, Zheng SH (2009) Spatial segmentation characteristic of focal mechanism of aftershock sequence of Wenchuan earthquake. Chin Sci Bull 54(16):2348–2354

Wang Q, Qiao XJ, Lan QG, Jeffrey F, Yang SM, Xu CJ, Yang YL, You XZ, Tan K, Chen G (2011) Rupture of deep faults in the 2008 Wenchuan earthquake and uplift of the Longmen Shan. Nat Geosci 4(9):634–640

Wu JP, Huang Y, Zhang TZ, Ming YH, Fang LH (2009) Aftershock distribution of the M_S8.0 Wenchuan earthquake and three dimensional P-wave velocity structure in and around source region. Chin J Geophys 52(2):320–328

Xu ZH, Yan M, Zhao ZH (1983) Evaluation of the direction of tectonic stress in north China from recorded data of a large number of small earthquakes. Acta Seismol Sin 5(3):268–279

Xu ZH, Wang SY, Huang YR, Gao AJ, Jin XF, Chang XD (1987) Detections of mean stress axes in southwestern China deduced from microearthquake data. Acta Seismol Sin 30(5):476–486

Xu ZH, Wang SY, Huang YR, Gao AJ (1989) The tectonic stress field of Chinese continent deduced from a great number of earthqaukes. Acta Geophys Sin 32(6):636–647

Xu XW, Wen XZ, Yu GH, Chen GH, Klinger Y, Hubbard J, Shaw J (2009) Coseismic reverse- and oblique-slip surface faulting generated by the 2008 M_W7.9 Wenchuan earthquake, China. Geology 37(6):515–518

Yi GX, Long F, Zhang ZW (2012) Spatial and temporal variation of focal mechanisms for aftershocks of the 2008 M_S8.0 Wenchuan earthquake. Chin J Geophys 55(4):1213–1227. doi:10.6038/j.issn.0001-5733.2012.04.017

Yu CQ, Tao K, Cui XF, Hu XP, Ning JY (2009) P wave first-motion focal mechanism solutions and their quality evaluation. Chin J Geophys 52(5):1402–1411

Yu HY, Tao K, Cai C, Zhang H, Ning JY, Wang YB (2013) Focal mechanism solutions of the tohoku-Oki earthquake sequence and their geodynamical implications. Chin J Geophys 56(8):2655–2669. doi:10.6038/cjg20130815

Zhang H, Ge ZX (2010) Tracking the rupture of the 2008 Wenchuan earthquake by using the relative back-projection method. Bull Seismol Soc Am 100(5B):2551–2560

Zhang PZ, Xu XW, Wen XZ, Ran YK (2008) Slip rates and recurrence intervals of the Longmen Shan active fault zone, and tectonic implications for the mechanism of the May 12 Wenchuan earthquake, 2008, Sichuan, China. Chin J Geophys 51(4):1066–1073

Zhang Y, Feng WP, Xu LS, Zhou CH, Chen YT (2009) Spatio-temporal rupture process of the 2008 great Wenchuan earthquake. Sci China Ser D 52(2):145–154

Zhang Y, Xu LS, Chen YT (2013) Rupture process of the Lushan 4.20 earthquake and preliminary analysis on the disaster-causing mechanism. Chin J Geophys 56(4):1408–1411

Zheng Y, Ma HS, Lv J, Ni SD, Li YC, Wei SJ (2009) Source mechanism of strong aftershocks ($M_S \geq 5.6$) of the 2008/05/12 Wenchuan earthquake and the implication for seismotectonics. Sci China Ser D 52(6):739–753

Zheng XF, Yao ZX, Liang JH, Zheng J (2010a) The role played and opportunities provided by IGP DMC of China National Seismic Network in Wenchuan Earthquake disaster relief and researches. Bull Seismol Soc Am 100(5B):2866–2872

Zheng Y, Ni SD, Xie ZJ, Lv J, Ma HS, Sommerville P (2010b) Strong aftershocks in the northern segment of the Wenchuan earthquake rupture zone and their seismotectonic implications. Earth Planets Space 62:881–886